Arab J Geosci (2015) 8:8999–9013
DOI 10.1007/s12517-015-1876-6

ORIGINAL PAPER

Links between host rock, water, and speleothems of Xueyu Cave in Southwestern China: lithology, hydrochemistry, and carbonate geochemistry

Kunyu Wu · Licheng Shen · Tingshan Zhang · Qiong Xiao · Aoyu Wang

Received: 5 December 2014 / Accepted: 1 March 2015 / Published online: 14 March 2015

Abstract A systemic study was conducted to understand the links between the host rock, water, and speleothems of Xueyu Cave in Southwestern China. An outcrop section of the host rock of Xueyu Cave was surveyed, the stratum that the host rock belongs to was subdivided into 11 lithofacies, and the Xueyu Cave is developed in the grainstone facies segment. Lithological characteristics and chemical components of the host rock indicate that its predominant mineral component is low magnesium calcite (LMC). To understand the hydrochemical characteristics of percolating water in Xueyu Cave, three drip water monitoring sites were taken to collect water samples for a whole monsoon year. The temperature (*T*), pH, electronic conductivity (EC), drip rate, Ca^{2+}, Mg^{2+}, Na^{+}, K^{+}, Ba^{2+}, Sr^{2+}, HCO_3^{-}, SO_4^{2-}, NO_3^{-}, Cl^{-}, partial pressure of CO_2 (pCO_2), saturation indexes, and precipitation rate of carbonate minerals were investigated monthly. The data reveals that the pH, EC, drip rate, Ca^{2+}, Mg^{2+}, HCO_3^{-}, pCO_2, saturation indexes, and precipitation rate of carbonate minerals exhibit seasonal variation; these are due to the seasonal change of precipitation and soil CO_2 concentration that are driven by monsoon climate. The petrological and geochemical characteristics of speleothems were also investigated, and results indicate that the main chemical and mineral components of speleothems are quite similar to the host rock; this is because the main material source of drip water and speleothems are governed by the host rock. This study reveals the main mineralogical and geochemical characteristics of host rock and speleothems, further discussing the seasonal variation of hydrochemical indexes of drip water. All these works will be helpful to more thoroughly understand the operation regularity of karst dynamic system (KDS) of the Xueyu Cave.

Keywords Calcite · Drip water · Speleothem · Karst dynamic system (KDS) · Mg/Ca · Xueyu Cave

Introduction

Typically, speleothems are secondary mineral deposits formed in a karstic cave (Moore 1952), and the mechanisms of speleothem growth can be summarized as mobilization processes by which surface-derived components are redistributed to the subsurface via downward percolation of fluids (Holland et al. 1964; Thrailkill 1971; Bar-Matthews et al. 1991). During the processes, a series of water–rock interaction will happen, and many kinds of minerals will form (Ford and Williams 2007; Tămas et al. 2011). As of 2011, more than 300 cave minerals have been noted (Onac and Forti 2011a, b). However, only three minerals (calcite, aragonite, and gypsum) can be considered common (Self and Hill 2003). Therefore, many studies relating to these minerals have been performed, finding that the formation and characteristics of speleothems are strongly impacted by the external environment (Bar-Matthews

K. Wu (✉) · T. Zhang
State Key Laboratory of Oil and Gas Reservoir Geology and Exploitation, Southwest Petroleum University, Chengdu 610500, People's Republic of China
e-mail: wukunyu1986@126.com

K. Wu · L. Shen · Q. Xiao · A. Wang
School of Geographical Sciences, Southwest University, Chongqing 400715, People's Republic of China

Q. Xiao
Karst Dynamics Laboratory, MLR and GZAR, Institute of Karst Geology, CAGS, Guilin 541004, People's Republic of China

A. Wang
Sichuan Earthquake Administrations, Chengdu 610041, People's Republic of China

et al. 1991; Fairchild et al. 2000; Frisia et al. 2002; Self and Hill 2003; Spotl et al. 2005; Oster et al. 2012). Geochemistry-based studies revealed the main control factors on chemical and mineralogical characteristics of speleothems, including cover conditions, organisms, temperature, Mg/Ca ratio of percolating pore fluids, partial pressure of CO_2 (pCO_2), evaporative conditions within a cave, etc. (Gascoyne 1983; Bar-Matthews et al. 1991; Fairchild et al. 2000; Contos et al. 2001; Forti 2001; Frisia et al. 2002; Self and Hill 2003; Cacchio et al. 2004; Spotl et al. 2005; Oster et al. 2012). In fact, all the control factors and water–rock interaction processes work together as a whole system. Therefore, Yuan et al. (2002) suggested a conceptual model as karst dynamic system (KDS) to represent the operating principles of the system (Fig. 1). The KDS is an open system in which the solid phase (carbonate host rock) acts as the source of most cations (Ca^{2+}, Mg^{2+}, Sr^{2+}, etc.) and a half of all bicarbonate radical in the liquid phase; hence, the host rock can strongly impact the characteristics of the solution (liquid phase) and speleothems. But the links between the host rock, percolating water, and speleothems did not receive enough attention, causing the understanding on operation regularity of KDS not thorough enough.

The studies on Xueyu Cave have been performed for a couple of years; the early studies mainly focused on the morphology and taxology of the speleothems (Zhu et al. 2004). To understand the impact of factors on the properties of speleothems and waters, the monitoring work on Xueyu Cave has started in recent years. The studies on hydrochemistry found that the hydrochemical indices of drip water and underground stream water in Xueyu Cave vary seasonally, whereas the reasons are still unclear (Pu et al. 2009; Xu et al. 2012). In addition, none of them paid attention to the petrological characteristics of the host rock and speleothems, and they also did not systemically discuss the links between the host rock, percolating water, and speleothems.

This study seeks to find out the control factors on properties of percolating water and speleothems and to reveal the links between the host rock, percolating water, and speleothems. The results and new insights on petrology and geochemistry will be helpful to better understand the operation regularity of KDS of Xueyu Cave system.

Study site description and geological setting

Xueyu Cave (29° 47′ 00″ N, 107° 47′ 13″ E; entrance elevation 233 m) is located in Fengdu County 180 km from Chongqing City (Fig. 2a). Similar to most of southern China, this region has a typical subtropical monsoon climate that features wet season (May to Oct.) and dry season (Nov. to Apr.) and has a multiyear average precipitation of approximately 1072 mm. Xueyu Cave extends along the strike of the host rock and is a typical underground watercourse canyon–type cave (Zhu et al. 2004). With downcutting of the subterranean stream, this cave forms a multilayer structure (Fig. 2c). The cave does not develop large chambers, which is also attributed to the intense downcutting. The thickness of the roof rocks of Xueyu Cave is over 150 m, and the mean internal temperature is ~17.2 °C. The main speleothems in Xueyu Cave include soda straw, stalactites, stalagmites, cave flags, cave shields, tower corals, rafts etc. (Fig. 2e–h). The dating data show that the age of studied speleothems in Xueyu Cave is ~3400± 25 years (unpublished age data were provided by Dr. Yang, test work were performed in the University of Minnesota).

The study region is located in the eastern Sichuan basin between Huaying Mountain and Xuefeng Mountain. This region deformed in the late Mesozoic and formed a series of multilayer detachment folds (Wang et al. 2010, 2012). The structural setting of the study area region is an anticline, and Permian strata form the core of which. Xueyu Cave is in the northwestern wing of the anticline. Based on the different lithological characteristics, five different lithostratigraphic units are subdivided (Fig. 2b), e.g., Lower Permian (P_1) limestone with argillaceous rock at the bottom, Upper Permian (P_2) siliceous limestone, Lower Triassic Feixianguan formation (T_1f) limestone with argillaceous rock at the base and silt rock at the top, Lower Triassic Jialingjiang Formation (T_1j)

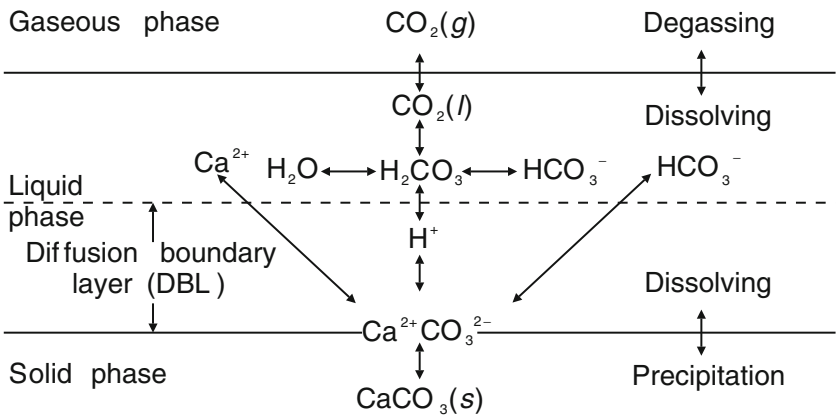

Fig. 1 Conceptual model of the karst dynamic system (KDS) (after Yuan et al. 2002)

dolomitic limestone with salt dissolution breccias at the top, and Middle Triassic Leikoupo Formation (T_2l) argillaceous limestone with silty shale embedded within.

The host rock of Xueyu Cave is Feixianguan formation that was deposited in the early Triassic, approximately 252.6± 0.2~245.2 Ma (Huang et al. 2006, 2008) with sedimentary environment of evaporite-carbonate platform (Zharkov and Chumakov 2001). Based on the investigation of outcrop section and specimens, the Feixianguan formation was subdivided into 11 lithofacies (Fig. 2d). The Xueyu Cave is developed in the grainstone facies segment; its roof and floor rocks are predominated by thick-bedded micrite and medium–thin-bedded argillaceous limestone, separately.

Methods

The morphology of the cave was surveyed using a laser rangefinder (LRF) and compass. The mineralogy and textures of the bedrock and speleothems were characterized using a polarized microscope.

To characterize the variation of main environmental and hydrochemical parameters, we selected three drip water monitoring sites (#1, #2, and #3 in Fig. 2) and sampled monthly during a monsoon year (post-monsoon season of May to Oct. and pre-monsoon season of Nov. to Apr.).

Temperature (T), pH, and electric conductivity (EC) were measured in situ using a sension made by Hach (USA) and bicarbonate (HCO_3^-) was tested in situ using a portable kit made by Merck (Germany). Their accuracies are T 0.1 °C, EC 1 μS/cm, pH 0.01, and HCO_3^- 0.1 mmol/L, respectively. Monthly drip water samples from three monitoring points (#1, #2, and #3) were collected in 50-mL polyethylene bottles and a small amount of nitric acid (1:1) was added in, and then the samples were stored at 5 °C for cation analysis. The samples for anion analysis were also collected in 50-mL polyethylene bottles without acidifying. To test the chemical components of limestone and speleothems, 0.5 g of solid material from each sample was digested with nitric acid (1:1) and then diluted to 100 mL with deionized water. The chemical components of the drip water and solid samples were determined by inductively coupled plasma optical emission spectrometry (ICP-OES) and ion chromatography with a detection precision of 0.001 mg/L.

Results and discussion

Lithology of host rock

The lithofacies segment that the Xueyu Cave is developed in were subdivided into four different lithofacies types, including micritic limestone, calcarenite, oolitic limestone, and calcirudite (Fig. 2d). To characterize the lithology of the rocks, thin sections were produced for mineralogy and texture observation; the microscopic photos for rocks are shown in Fig. 3.

The micritic limestone is characterized in micro-crystalline texture and lime mud matrix, and it also contains some metallic minerals and clay minerals which are characterized by a brown to black color (Fig. 3(a, b, b+)). This rock is approximately 10 m in thickness and is sandwiched in the segment of grainstone lithofacies.

Except the micritic limestone, the total thickness of the other three rocks is over 50 m, which forms the main body of the grainstone lithofacies segment. The oolitic limestone consists of oolite grains in size of 0.5~1.0 mm and granular calcite cements; subhedral quartz characterized by a six-sided prismatic shape and grayish white interference color can also be found occasionally (Fig. 3(c, d, d+)). Figure 3(e, f, f+) presents the texture and mineral components of calcarenite; the images demonstrate that their predominant constituents are silt to fine sand-sized intraclasts. Like the oolitic limestone, the cements of the calcarenite also mainly consist of granular calcite. Figure 3(g, h, h+) shows that the calcirudite is made up of gravel-sized (>2 mm) and some sand-sized micritic limestone grains, the cements of which also consists of isometric granular calcite cements.

Based on the microscopic images, it is easy to find that all grainstones (oolitic limestone, calcarenite, and calcirudite) have a high original porosity of proportion over 40 %, which provides enough space for crystal growth; hence, the cements of the stones consist of granular calcite. In addition, the images also present that the calcite crystals of cements are of equant morphology, indicating a little difference in surface energy of the calcite crystal planes during the crystallization processes in a diagenetic fluid of low magnesium concentration (Lahann 1978). Indeed, the calcite of isometric granular texture is the most common cement for limestone that formed in a diagenetic environment of low magnesium content, such as the freshwater phreatic diagenetic environment (Longman 1980; Scholle and Ulmer-Scholle 2003; Huang 2010). Therefore, the universal existence of calcite cements of isometric granular morphology in the host rocks of Xueyu Cave indicates that the magnesium content in their predominant mineral components are very likely to be low.

Chemical composition of host rock

To quantitatively characterize the chemical composition and to provide support to the inference about the mineral compositions of the host rock, ten host rock samples were chosen for chemical component analysis. The results demonstrate that the Ca content of these rocks ranges from 9.58 to 9.94 mol/kg, and their Mg content ranges from 0.04 to 0.36 mol/kg (Table 1). In general, calcites have a magnesium carbonate molar ratio of less than 4 % (Mg/Ca <4 %) can be classified

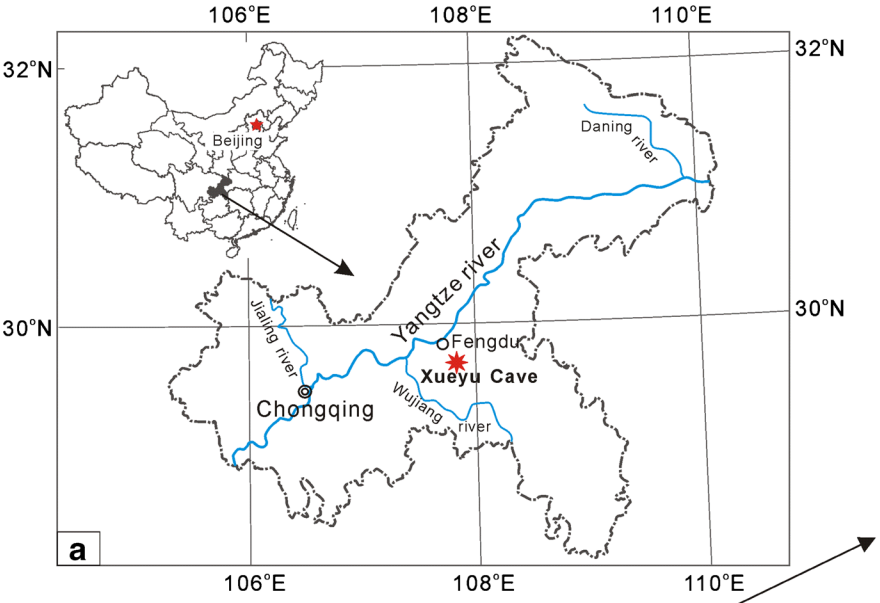
106°E
108°E
110°E
32°N
30°N
Beijing
Daning river
Yangtze river
Jialing river
Fengdu
Xueyu Cave
Chongqing
Wujiang river
a

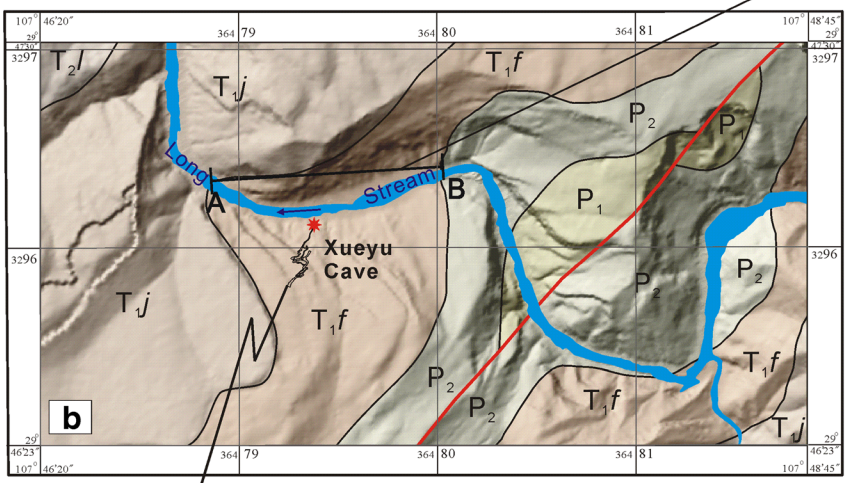
T2l
T1j
T1f
P2
P1
Long Stream
A
B
Xueyu Cave
b

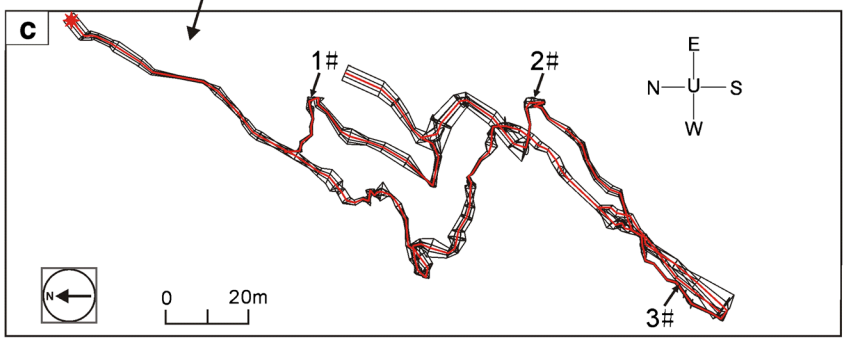
c
1#
2#
3#
E
N
S
W
0
20m


e


f
g


h

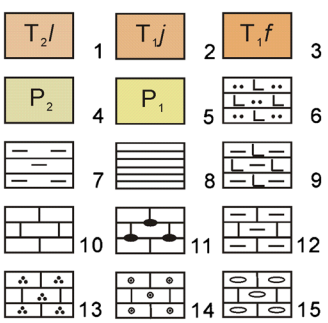
T2l 1
T1j 2
T1f 3
P2 4
P1 5
6
7
8
9
10
11
12
13
14
15

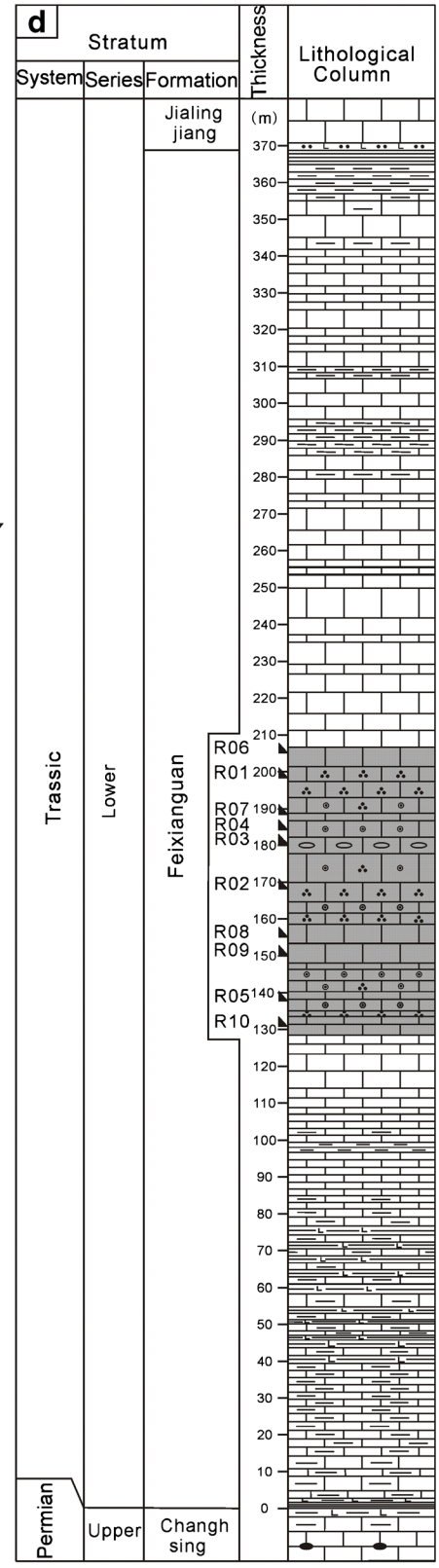
d
Stratum
System
Series
Formation
Thickness
(m)
Lithological Column
Trassic
Lower
Permian
Upper
Jialing jiang
Feixianguan
Changh sing
R06
R01
R07
R04
R03
R02
R08
R09
R05
R10

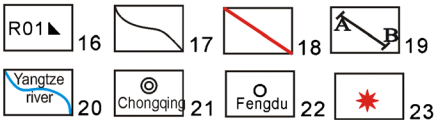
R01 16
17
18
A
B
19
Yangtze river 20
Chongqing 21
Fengdu 22
23

◀ **Fig. 2** Location, geological setting, and speleothems of Xueyu Cave. **a** location of the study site; **b** geological setting of the study site; **c** morphology of Xueyu Cave; *1#*, *2#*, and *3#* are drip water monitoring sites; **d** host rock lithofacies division; **e** cave flags and stalagmites; **f** soda straw; **g** cave shield; **h** flowstones and stalagmites; *1* Middle Triassic Leikoupo Formation, *2* Lower Triassic Jialingjiang Formation, *3* Lower Triassic Feixianguan Formation, *4* Upper Permian series, *5* Lower Permian series, *6* calcareous silt rock, *7* argillaceous rock, *8* shale, *9* calcareous argillaceous rock, *10* micritic limestone, *11* siliceous limestone, *12* argillaceous micritic limestone, *13* calcarenite, *14* oolitic limestone, *15* calcirudite, *16* sample locations and ID, *17* conformity stratigraphic boundary, *18* fault, *19* location of measured geological section, *20* river/stream and its name, *21* city, *22* county, *23* location of the cave mouth; the Xueyu Cave is developed in the grainstone facies segment of gray shadow in (**d**)

as the low magnesium calcite (LMC) (Stanley et al. 2002). The magnesium and calcium molar ratio (Mg/Ca) of the limestone samples ranges from 0.59 to 3.53 % (Table 1), indicating their predominant carbonate mineral components belong to LMC, which is consistent with the inference about the host rock's mineral composition.

Besides calcium and magnesium, the other contents of the rocks are much lower. Their Ba, Sr, Fe, and Mn contents range form 83.47 to 280.35×10^{-6}, from 8.10 to 465.74×10^{-6}, from 102.02 to 1840.38×10^{-6}, and from 5.81 to 65.43×10^{-6}, respectively.

In addition, the calcium content of samples demonstrates a good negative correlation with the magnesium content

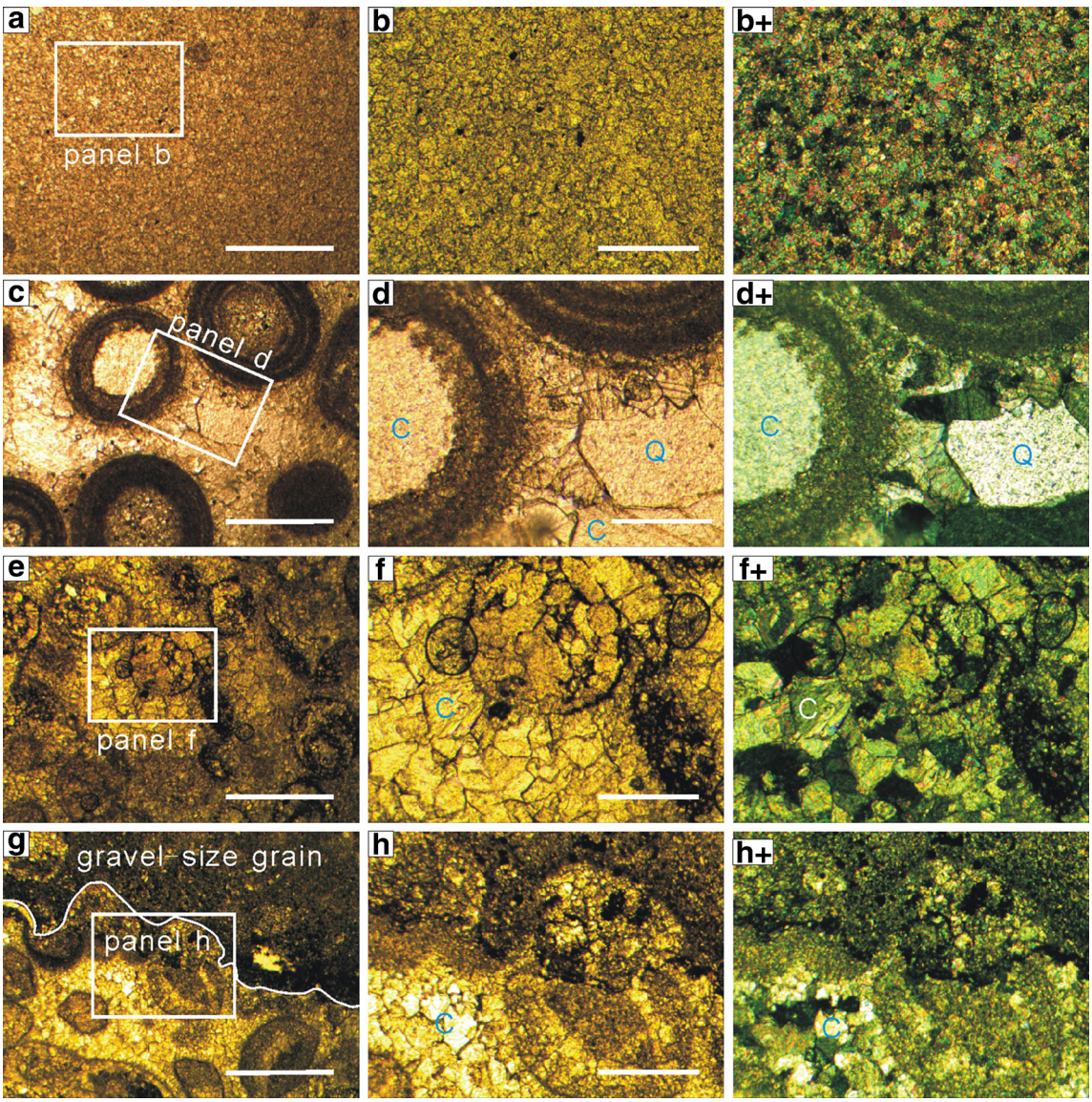

Fig. 3 Thin slice images for the bedrock of the Xueyu Cave system. *a*, *b*, *b+* are micritic limestone that consists of very tiny calcite crystals with size <0.01 mm; *c*, *d*, *d+* are oolitic limestone with granular calcite cements, and subhedral quartz can be found occasionally; *e*, *f*, *f+* are calcarenite that consists of silt to fine sand-sized intraclasts with granular calcite cements; *g*, *h*, *h+* are calcirudite that consists of gravel-sized (>2 mm) and some sand-sized carbonate grains with granular calcite cements. *Plus sign* means the images were taken with cross-polarized light. *Scale bars*=0.5 mm (a, c, e, and g) and 0.1 mm (b, d, f, and h). *C* calcite, *Q* quartz

Table 1 Chemical composition of host rocks

ID	Rock type	Ca mol/kg	Mg	Mg/Ca $\times10^{-2}$	Ba $\times10^{-6}$	Sr	Fe	Mn
R1	Calcarenite	9.94	0.06	0.59	29.05	235.66	102.02	5.81
R2	Calcarenite	9.76	0.24	2.48	465.74	205.81	1262.89	45.20
R3	Calcirudite	9.83	0.18	1.86	59.10	181.19	792.22	19.44
R4	Oolitic limestone	9.77	0.24	2.48	11.33	216.47	818.62	32.04
R5	Oolitic limestone	9.87	0.14	1.40	16.66	83.47	232.12	32.40
R6	Micritic limestone	9.90	0.10	1.05	50.75	117.66	377.93	23.57
R7	Micritic limestone	9.89	0.12	1.20	8.10	158.35	343.15	18.71
R8	Micritic limestone	9.90	0.10	1.03	11.58	257.91	185.74	11.96
R9	Micritic limestone	9.85	0.11	1.17	148.77	280.35	1840.38	65.43
R10	Micritic limestone	9.58	0.34	3.53	44.06	86.06	134.94	6.43

(Fig. 4), and the samples have lower Mg content than that of modern marine carbonate, indicating massive Mg has migrated out of the original carbonate minerals during the meteoric water diagenetic environment (Huang 2010).

Drip water environmental parameters

The analysis data for drip waters exhibit that the temperature of all samples ranges from 16.7 to 19.3 and does not change much intra-annually, whereas the other environmental parameters are quite variable in different monitoring sites and seasons. Their pH ranges from 7.25 to 8.33 show weakly alkaline in nature, which is a typical pH distribution interval (6.5~8.9) of waters in a karst region (Ford and Williams 2007). The pH of waters at sites #2 and #3 is higher than that at site #1; in addition, the pH in dry season is higher than that in wet season with mean values of 7.49 and 7.93, separately (Fig. 5) (Table 2). The EC ranges from 254.0 to 1507.0 μS/cm, which at site #1 is much higher than that at sites #2 and #3, although the regularity of the EC variation is not as clear as that of the pH. We can also find that the EC varies seasonally; indeed, the mean values of EC in dry season and wet season are 673.9 and 576.4 μS/cm, respectively (Fig. 5) (Table 2). Generally, due to the impact of monsoon precipitation, the drip rate in post-monsoon season is much higher than that in pre-monsoon season, and this trend is presented clearly in Fig. 5. Besides seasonal variation, the drip rate is also quite variable in

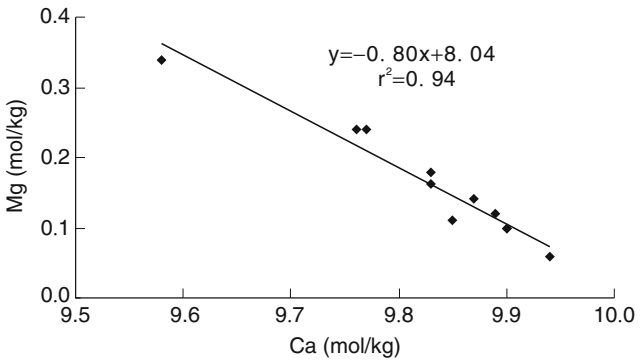

Fig. 4 Correlation between Mg and Ca content

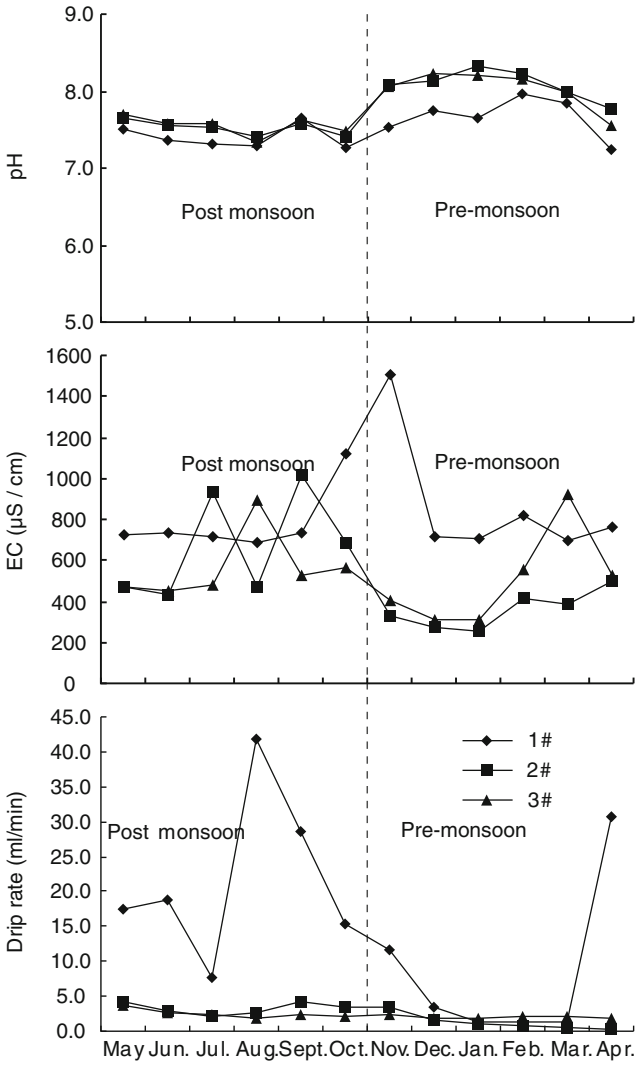

Fig. 5 Environmental parameters variation for drip waters

Table 2 Environmental parameters and chemical components of drip water

Sample sites	Month	pH	T (°C)	EC (μS/cm)	Drip rate (mL/min)	Ca^{2+} (mg/L)	Mg^{2+}	Na^{+}	K^{+}	
#1	May	7.50	17.5	725.0	17.5	162.50	3.65	1.68	0.83	
	Jun.	7.37	17.7	733.0	18.8	167.93	3.64	1.65	0.84	
	Jul.	7.31	17.5	715.0	7.6	169.65	3.90	0.82	0.36	
	Aug.	7.30	18.0	690.0	41.7	165.66	3.88	0.88	0.88	
	Sept.	7.64	17.5	732.0	28.5	173.90	3.85	0.79	0.38	
	Oct.	7.26	17.5	1122.0	15.3	191.00	3.91	0.76	0.41	
	Nov.	7.54	17.4	1507.0	11.6	219.88	4.05	1.17	0.69	
	Dec.	7.74	17.4	713.0	3.6	184.98	4.35	0.90	0.42	
	Jan.	7.64	18.1	707.0	1.4	162.95	4.09	0.82	0.50	
	Feb.	7.97	17.1	817.0	1.3	157.40	4.45	0.79	0.49	
	Mar.	7.84	17.3	698.0	1.2	167.51	4.12	0.96	0.61	
	Apr.	7.25	18.5	763.0	30.8	179.42	4.07	0.96	0.40	
#2	May	7.66	18.6	470.0	4.3	93.51	6.89	1.78	1.10	
	Jun.	7.55	18.2	432.0	2.9	82.02	6.77	1.76	1.09	
	Jul.	7.54	18.0	933.0	2.2	83.14	7.38	0.93	0.58	
	Aug.	7.41	19.3	473.0	2.6	86.25	7.65	0.89	1.05	
	Sept.	7.58	18.2	1018.0	4.2	88.92	7.35	0.93	0.74	
	Oct.	7.41	18.2	690.0	3.6	122.96	7.47	0.88	0.65	
	Nov.	8.09	18.2	334.0	3.4	88.25	7.27	1.38	0.97	
	Dec.	8.14	18.3	269.0	1.6	47.59	7.68	0.94	0.63	
	Jan.	8.33	18.5	254.0	1.0	30.60	7.87	0.91	0.57	
	Feb.	8.24	18.3	413.0	0.7	35.26	7.83	0.90	0.59	
	Mar.	8.00	18.5	389.0	0.4	49.07	7.87	1.16	0.67	
	Apr.	7.78	18.5	499.0	0.3	88.96	9.50	1.38	0.76	
#3	May	7.70	17.3	472.0	3.6	89.97	8.09	1.87	1.09	
	Jun.	7.58	17.8	456.0	2.7	79.92	8.25	1.92	1.12	
	Jul.	7.59	16.7	480.0	2.4	84.18	8.97	1.13	0.63	
	Aug.	7.34	18.6	892.0	1.9	95.41	9.02	1.30	2.41	
	Sept.	7.63	16.9	531.0	2.3	94.73	9.28	3.25	1.34	
	Oct.	7.48	16.8	566.0	2.1	118.35	9.07	1.12	0.63	
	Nov.	8.06	17.2	403.0	2.3	89.35	8.70	1.56	1.19	
	Dec.	8.24	17.7	307.0	1.9	61.95	9.58	1.10	0.72	
	Jan.	8.21	18.5	308.0	1.8	43.07	9.24	1.06	0.47	
	Feb.	8.16	18.1	551.0	2.2	42.71	9.17	1.10	0.75	
	Mar.	7.98	18.6	919.0	2.1	56.02	8.99	1.14	0.61	
	Apr.	7.55	18.9	525.0	1.7	101.07	10.18	1.66	1.39	
Sample sites	Month	Sr^{2+} (mg/L)	HCO_3^-	Cl^-	SO_4^{2-}	NO_3^-	TDI	SIa	SIc	Log (pCO_2)
#1	May	0.06	451.4	1.81	51.26	0.89	508.47	0.66	0.81	−1.83
	Jun.	0.06	451.4	2.62	57.74	2.06	516.77	0.54	0.69	−1.70
	Jul.	2.15	475.8	2.01	54.76	2.09	538.38	0.50	0.65	−1.62
	Aug.	2.13	427.0	1.74	19.98	1.61	454.56	0.46	0.61	−1.65
	Sept.	2.20	427.0	1.27	45.12	1.13	478.61	0.80	0.95	−2.00
	Oct.	2.18	439.2	1.86	61.74	0.86	507.33	0.47	0.61	−1.61
	Nov.	2.13	512.4	2.98	34.60	2.33	557.29	0.86	1.01	−1.83
	Dec.	2.16	427.0	1.90	61.66	0.65	495.81	0.91	1.06	−2.11
	Jan.	2.01	439.2	1.71	54.03	0.89	500.14	0.79	0.94	−1.99
	Feb.	3.56	457.5	1.78	52.94	1.62	520.56	1.10	1.25	−2.31
	Mar.	1.95	457.5	1.72	52.73	1.11	517.79	1.00	1.15	−2.18

Table 2 (continued)

	Apr.	2.07	451.4	1.64	66.69	1.73	525.22	0.46	0.60	−1.58
#2	May	0.14	317.2	1.61	25.55	2.01	349.91	0.49	0.64	−2.13
	Jun.	0.13	250.1	1.82	28.78	2.26	286.31	0.23	0.38	−2.12
	Jul.	4.85	274.5	1.94	29.65	2.58	315.46	0.26	0.41	−2.07
	Aug.	4.93	262.3	1.88	30.64	2.80	304.74	0.15	0.29	−1.96
	Sept.	4.45	268.4	0.99	33.27	1.71	310.97	0.32	0.47	−2.12
	Oct.	4.90	280.6	1.11	30.68	2.17	321.37	0.29	0.44	−1.94
	Nov.	4.15	183.0	2.78	17.40	3.09	213.96	0.67	0.81	−2.81
	Dec.	4.31	146.4	1.36	31.03	3.06	188.89	0.38	0.53	−2.94
	Jan.	4.53	128.1	1.39	32.11	4.52	173.31	0.33	0.48	−3.19
	Feb.	4.56	176.9	1.38	30.96	2.48	219.07	0.43	0.58	−2.96
	Mar.	4.70	176.9	1.40	31.19	2.58	219.25	0.33	0.48	−2.72
	Apr.	5.77	183.0	1.77	38.92	6.31	238.31	0.36	0.51	−2.49
#3	May	0.17	274.5	1.81	31.08	4.16	315.20	0.44	0.59	−2.24
	Jun.	0.18	256.2	2.04	35.01	4.69	301.53	0.25	0.40	−2.14
	Jul.	5.98	268.4	3.16	39.95	12.71	332.40	0.28	0.43	−2.14
	Aug.	6.35	262.3	2.68	38.68	5.52	319.50	0.10	0.25	−1.89
	Sept.	6.38	280.6	1.67	43.94	5.36	343.03	0.38	0.53	−2.17
	Oct.	6.38	305.0	2.06	38.87	4.26	358.72	0.35	0.50	−1.98
	Nov.	5.73	213.5	2.93	21.36	3.97	251.60	0.68	0.83	−2.72
	Dec.	5.57	128.1	2.61	38.75	4.50	182.48	0.51	0.66	−3.11
	Jan.	5.40	146.4	1.93	37.94	5.33	199.78	0.40	0.55	−3.02
	Feb.	5.22	170.8	1.59	35.93	2.91	219.60	0.41	0.56	−2.90
	Mar.	5.70	170.8	1.86	36.41	3.67	220.85	0.35	0.50	−2.72
	Apr.	6.74	268.4	1.59	40.33	3.04	323.56	0.34	0.49	−2.09

SIa saturation index of aragonite, *SIc* saturation index of calcite, *EC* electric conductivity, *TDI* total dissolved ion, *Log(pCO_2)* partial pressure of carbon dioxide

different sites, site #1 has much higher drip rate than that at sites #2 and #3 (Table 2).

Major ion chemistry of drip water

In general, Ca^{2+} and HCO_3^- are the predominant cation and anion in karst waters (Yuan et al. 2002; Ford and Williams 2007), and the situation for drip waters in Xueyu Cave is certainly the same. The concentration of Ca^{2+} ranges from 30.60 to 219.88 mg/L and HCO_3^- ranges from 128.1 to 512.4 mg/L; they approximately account for 84 and 90 % of the total cations and total anions in molar ratio, respectively (Table 2). In addition, the Ca^{2+} and HCO_3^- in drip waters at sites #2 and #3 exhibit obviously seasonal variation, the concentration of which is higher in post-monsoon season than that of pre-monsoon season (Fig. 6). Besides Ca^{2+}, there are four other cations, including Mg^{2+}, Na^+, K^+, and Sr^{2+}, that can be detected in the waters. The abundance of all cations are $Ca^{2+}>Mg^{2+}>Sr^{2+}>K^+>Na^+$. Though Mg^{2+} concentration in drip waters does not show any remarkable variation. Its values in post-monsoon season are also a little higher than that in pre-monsoon season (Fig. 6). Except HCO_3^-, the other anions do not show any seasonal variation, and the abundance of anions are $HCO_3^->SO_4^{2+}>NO_3^->Cl^-$. The total dissolved ion (TDI) concentration of all water samples ranges from 173.31 to 557.29 mg/L, and drip waters at site #1 have higher TDI than that at sites #2 and #3. Because Ca^{2+} and HCO_3^- are the main ions in the waters, TDI exhibits very similar trend to them (Fig. 6).

Based on hydrochemical data, all water samples are classified using Piper plot (Piper 1944), and all samples are representing in Ca–HCO_3 facies (Fig. 7). Due to the enrichment of LMC in the host rock, this type of water mainly results from the dissolution of LMC by water–rock interaction. Gibbs (1970) suggested that the relative importance of the major natural mechanisms controlling groundwater chemistry can be characterized using a simple plot of total dissolved solid (TDS) versus the weight ratio of $Na^+/(Na^+ + Ca^{2+})$. Therefore, Gibbs plot was employed in this study to understand and differentiate the processes that control the drip water chemistry. In the plot, all samples collected in both pre-monsoon and post-monsoon seasons fall in the rock weathering dominance field, suggesting that the weathering of carbonate host rocks primarily controls the ion chemistry of drip waters (Fig. 8).

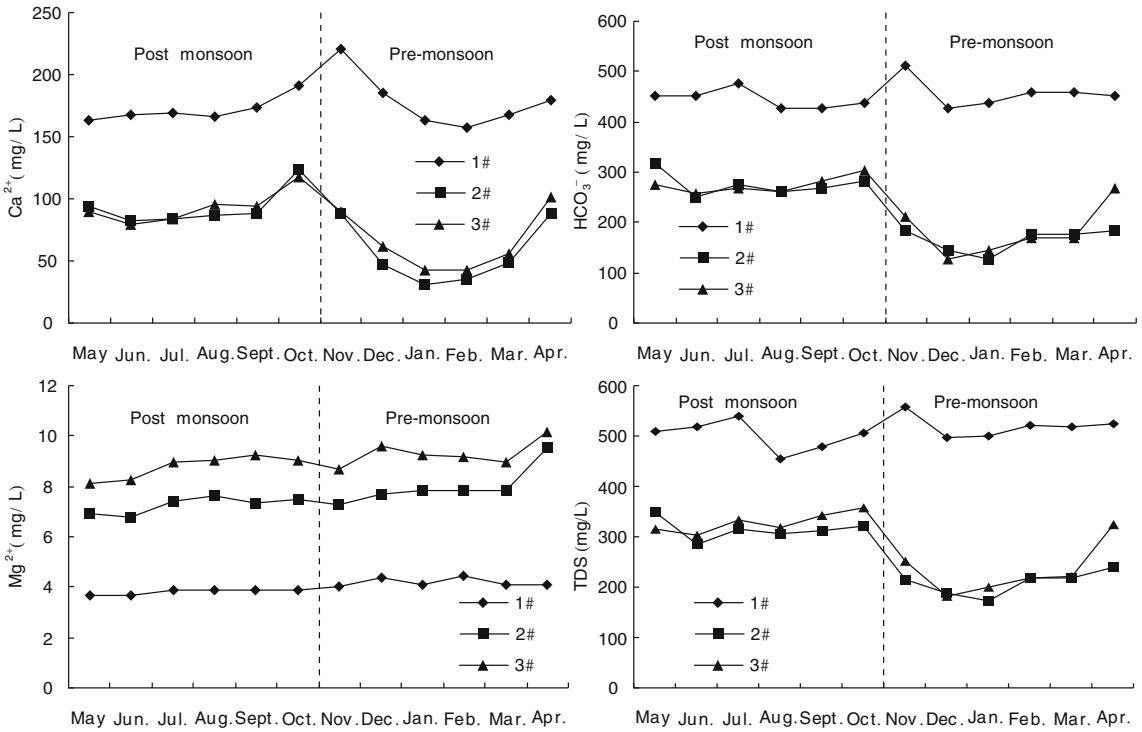

Fig. 6 Seasonal trend of Ca, Mg, HCO_3^-, and TDS for drip waters

Mg/Ca and saturation index of carbonate mineral

Magnesium has long been considered as the principal inorganic modifier of calcite morphology in natural waters (Folk 1974; Lahann 1978; Davis et al. 2004), and variation of Mg/Ca ratio in mother liquor from which the mineral precipitates is usually considered as an important indicator for prediction on mineral facies. Therefore, study on Mg/Ca ratio in drip waters is very important for understanding the mineralogy of speleothems.

Generally, water residence time controls the amount of water–rock interaction that occurs, with drier intervals resulting in longer residence time, more extensive water–rock interaction, and higher Mg/Ca (Musgrove and Banner 2004). The Mg/Ca ratio of the drip waters ranges from 0.03 to 0.43 in molar ratio, which exhibits a seasonal variation and has higher values in pre-monsoon season than that in post-monsoon season at sites #2 and #3. In addition, the Mg/Ca ratio at sites #2 and #3 also presents a seasonal variation with a trend of rising firstly and then decreasing in pre-monsoon season (Fig. 9). The Mg/Ca ratio at site #1 shows a relatively stable variation trend, the mean value of which in pre-monsoon season is just a little higher than that in post-monsoon season. To evaluate the impact of Ca and Mg on Mg/Ca ratio, linear regression

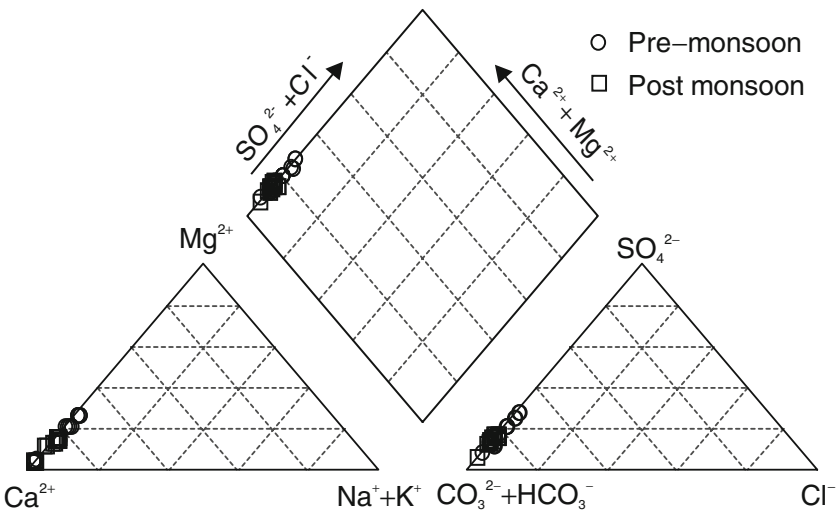

Fig. 7 Piper plot for water samples

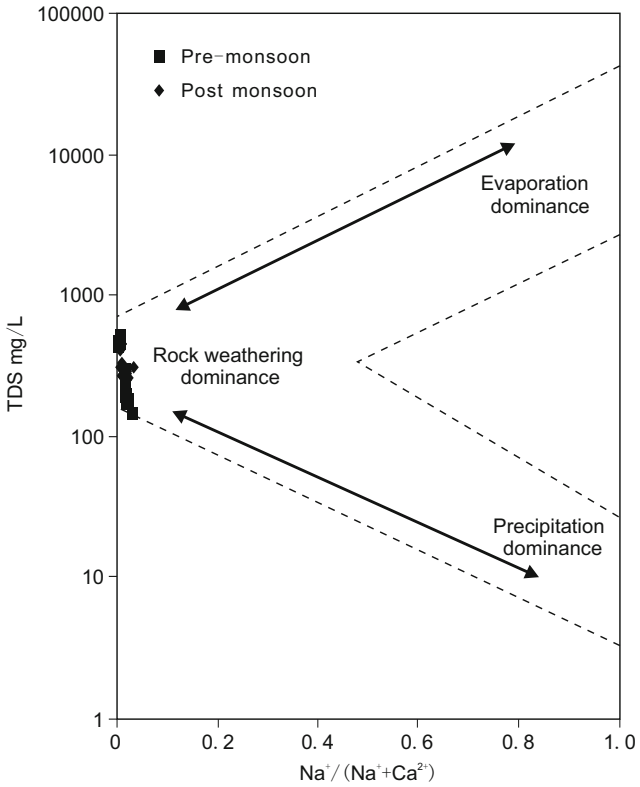

Fig. 8 Gibbs plot for water samples

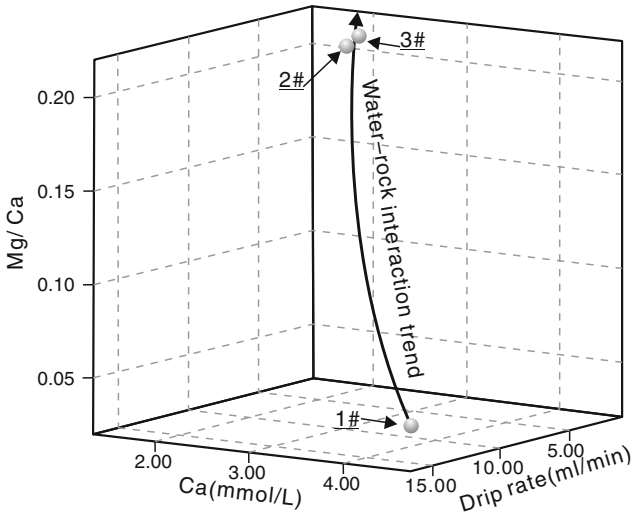

Fig. 10 Correlation among Ca, Mg/Ca, and drip rate in drip waters at different sites

analysis was applied to characterize the correlation between Mg/Ca, Ca, and Mg. The results show that the Mg/Ca ratio has a very good negative correlation with the Ca concentration and shows a weak positive correlation with Mg concentration (Fig. 9), indicating the Ca concentration in drip waters plays as a control factor on Mg/Ca ratio. Besides seasonal variation, the value of Mg/Ca ratio is different in different sites. Figure 10 demonstrates the correlation among Ca, Mg/Ca, and drip rate at different monitoring sites. The drip water at site #1 has the lowest Mg/Ca ratio and the highest Ca concentration and drip rate, indicating a weak water–rock interaction and short residence time of water, whereas sites #2 and #3 drip waters have higher Mg/Ca ratio and lower drip rate, indicating relatively extensive water–rock interaction by longer residence time.

To determine the chemical equilibrium between minerals and waters, saturation indexes of carbonate minerals were calculated using PHREEQC software package (Parkhurst and Appelo 1999). The calculated values of calcite (SIc) and aragonite (SIa) are both supersaturated (Table 2), indicating they are very likely to precipitate. The box plot shows the saturation index of carbonate minerals in drip waters at site #1 is higher than that at the other two sites and the values for waters at the three sites are different (Fig. 11), which may indicate the different water–rock interaction amounts and different flow paths of percolating waters. Besides, there are some outlier saturation index values in drip water at sites #2 and #3, which may also be caused by different water–rock interaction intensities in different seasons.

In caves, the outgassing of CO_2 drives the carbonate equilibrium (Toran and Roman 2006); accompanying with the degassing of CO_2, the pCO_2 in the waters will decrease and result in decrease of hydrogen ion activity, which leads to the pH increase further moves the reaction towards precipitation

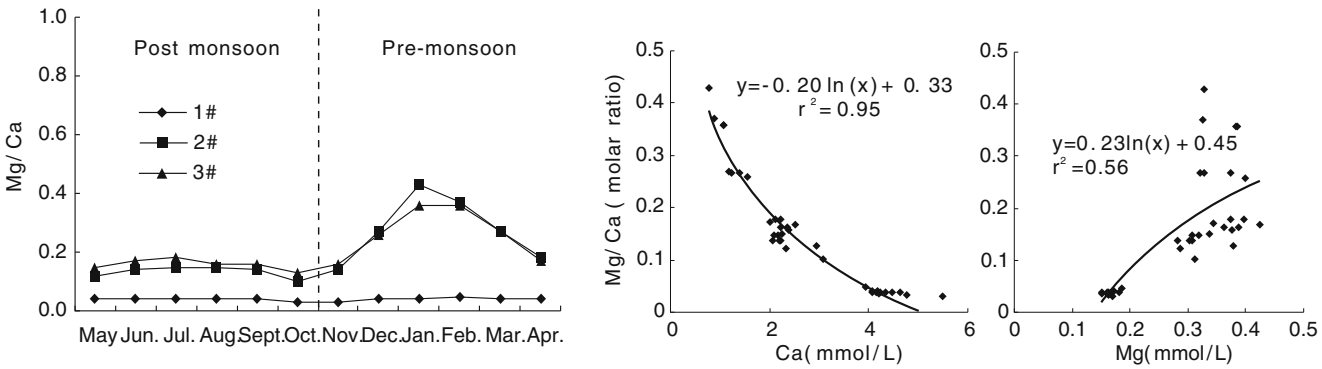

Fig. 9 Seasonal variation and correlation between Mg/Ca and Ca, Mg/Ca, and Mg for drip waters

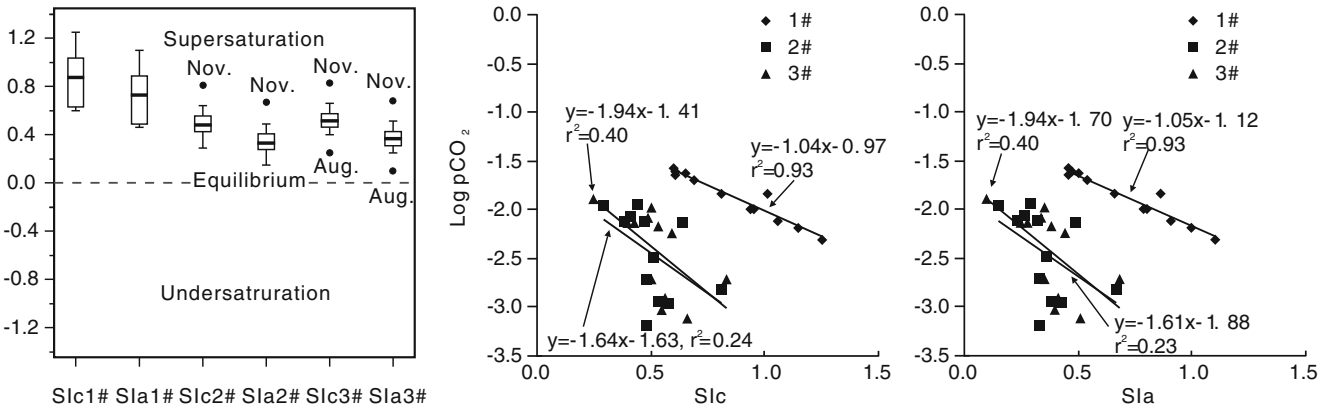

Fig. 11 Box plot for saturation index of carbonate minerals and correlation between log(pCO_2) and saturation index of carbonate minerals

of calcite. Therefore, the saturation index values of carbonate minerals are higher in pre-monsoon than those in post-monsoon season. Figure 11 demonstrates that saturation index has a negative correlation with log(pCO_2), but the correlation coefficient at different sites is different; the correlation coefficient at site #1 is very good, whereas coefficient values at sites #2 and #3 are weaker, indicating that a relatively higher drip rate (site #1) is good for promoting the carbonate minerals reaching supersaturation in Xueyu Cave.

Mineralogy and chemical composition of speleothems

Although calcite and aragonite are both in supersaturated stage, the high saturation index values do not mean both minerals can precipitate from the solution. Folk (1974) noted that magnesian calcite, aragonite, and dolomite only form in a fluid of high Mg/Ca (2:1~10:1) ratios, generally causing elongation of crystals parallel to the *c*-axis, resulting in acicular or fibrous habits. Conversely, low Mg/Ca ratio (1:10~2:1) solutions yield the rhombic forms of low magnesium calcite. In cave environment, Gonzalez and Lohmann (1987) observed that aragonite is precipitated when the fluid Mg/Ca ratio exceeds 1.5. Although the Mg/Ca ratio of drip waters in Xueyu Cave varies seasonally and the values in pre-monsoon season are much higher than that in post-monsoon season, the highest value does not exceed 0.5. Therefore, according to the previous experiences on Mg/Ca ratio impact to mineralogy of carbonate minerals, the minerals precipitating from the drip waters in Xueyu Cave are likely to be LMC.

To prove our hypothesis, the morphology and chemical compositions of speleothems are studied. The microscopic images of the drip water sediments demonstrate their crystal morphology are mainly of rhombic forms and apparently helical stripes that formed by screw dislocations (Fig. 12a, b). Davis et al. (2004) made in situ observations of calcite crystallization onto a seed crystal within a fluid cell in a continuous flow-through geometry using an atomic force microscope (AFM); the results show that the calcite precipitated from Mg-free solution is of symmetrically rhombic shape and straight step edges (Fig. 12c). When some impurity of Mg^{2+} was add into the solution (Mg/Ca=0.6), the step edges began to roughen (Fig. 12d) and the morphology of the calcite was definitely changed. Although the step edges of calcite crystals that precipitated from the drip water are not as straight as the crystals formed in Mg-free solutions, their external morphology are of better symmetry than that of the image in Fig. 12c, indicating the Mg/Ca ratios in drip waters are higher than zero and lower than 0.6. This is according to the investigation results of the Mg/Ca ratios in drip waters in Xueyu Cave. Besides the sediments that precipitate from drip waters at present, the speleothems that formed before also have good rhombic forms; Fig. 12e~h shows clear (1011) and ($01\overline{1}1$) cleavage faces and a good rhombic shape, these crystallographic characteristics typically belong to low magnesium calcite.

Because a lower Mg content in solution is favorable to calcite precipitation and fast sideward growth (Folk 1974; Frisia et al. 2002; Choudens-Sanchez and Gonzalez 2009), the calcite of speleothems in Xueyu Cave are usually of large size and good idiomorphology (Fig. 12i, j). Microscopic images show that the calcites of speleothems are formed in three different periods and characterized by different optical characteristics, shapes, and sizes. The calcite crystals formed in the first period have a euhedral shape and big size; the crystals formed in the second period have a subhedral shape and smaller size than the euhedral ones; the crystals formed in the third period are of a xenomorphic shape and the smallest size and in filling in the intergranular or intragranular pores (Fig. 12k, l).

The Ca and Mg abundance of speleothems is similar to that of the host rock, and their Mg/Ca mole ratios range from 0.25 to 3.27 (Table 3); thus, the calcites of the speleothems belong to LMC. The chemical data of Ca and Mg content provides hard evidence to support the prediction of mineral components which is based on their crystallographical characteristics. The abundance of trace elements of speleothems is different from that of the host rock. The Ba abundance of speleothems ranges from 17.19 to 484.44×10^{-6} with a mean

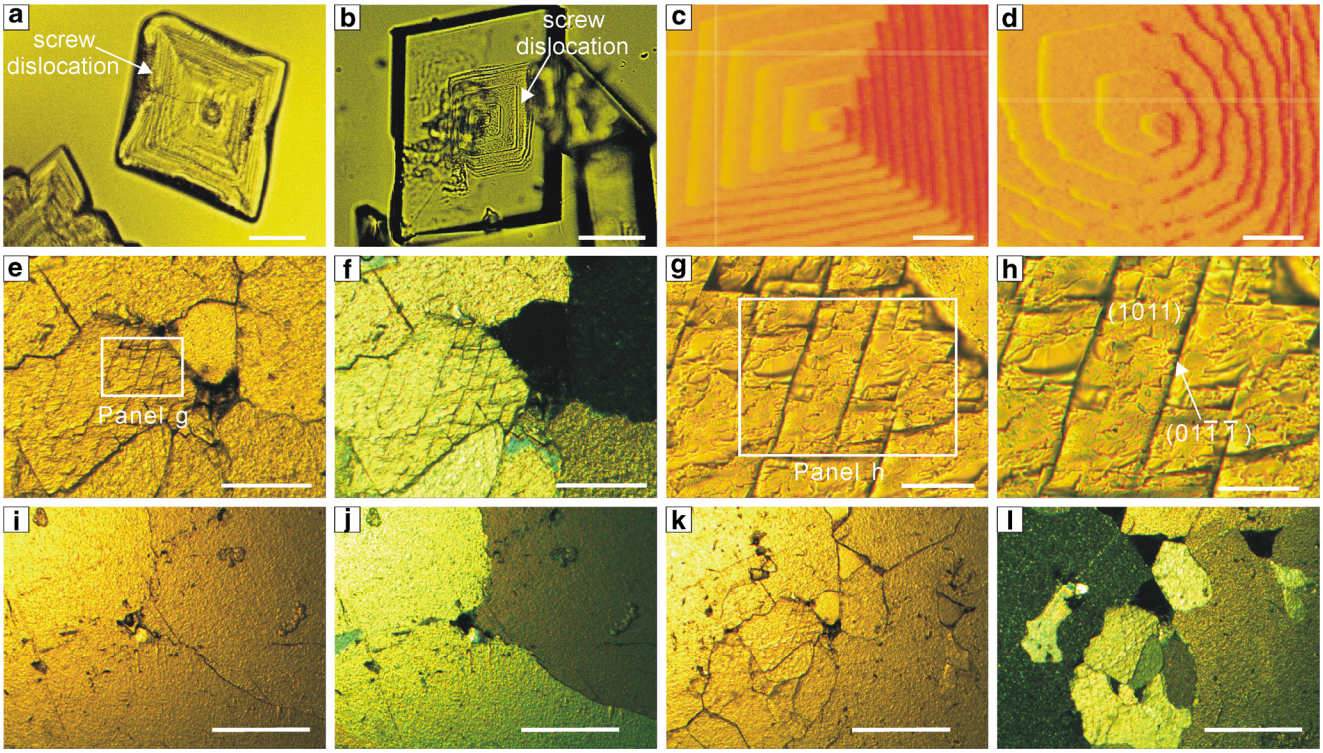

Fig. 12 Microscopic images of speleothems. **a**, **b** The drip water sediments' crystals of rhombic forms and screw dislocation; **c**, **d** The morphology of growth hillocks of calcite precipitate from Mg-free solution (Mg/Ca=0) and low Mg/Ca ratio (Mg/Ca=0.6) solutions (after Davis et al. 2004); **e~h** The characteristics of the cleavages of calcite in speleothems, two cleavage faces as (1011) and (01$\bar{1}\bar{1}$) can be found; **i~l** the size and optical characteristics of calcite formed in different periods. **a**, **b**, **e**, **g**, **h**, **i**, **k** were taken with plane polarized light; **c**, **d** were investigated using an atomic force microscope (AFM); **f**, **j**, **l** were taken with cross polarized light; *scale bars*=20 μm (**a**, **b**, **g**, and **h**), 300 nm (**c d**), 100 μm (**e**, **f**), and 0.5 mm (**i~l**)

value of 138.05×10^{-6} which is higher than that of the host rock with a mean value of 84.51×10^{-6}, whereas Sr, Fe, and Mn have mean values of 111.57×10^{-6}, 22.38×10^{-6}, and 2.20×10^{-6}, respectively. These values are all lower than that of the host rock. The differences may be also caused by the water–rock interaction between liquid and different host rocks that happened during the percolating processes.

Links between the host rock, water, and speleothems

Because the KDS is an open system (Yuan et al. 2002), its operation can be impacted by many environmental factors, including geological setting, climate, biology, etc. In this study, we focused on discussing links between the host rock, drip water, and speleothems in Xueyu Cave system on lithology, hydrochemistry, and carbonate geochemistry.

Table 3 Chemical compositions of speleothems

ID	Speleothem type	Ca mol/kg	Mg	Mg/Ca $\times10^{-2}$	Ba $\times10^{-6}$	Sr	Fe	Mn
S1	Soda straw	9.73	0.32	3.27	85.30	53.75	22.93	1.28
S2	Stalagmite	9.78	0.23	2.37	81.38	14.00	23.50	2.25
S3	Flowstone	9.91	0.09	0.89	17.19	153.69	16.50	1.22
S4	Soda straw	9.89	0.11	1.07	484.44	169.41	25.34	1.56
S5	Stalactite	9.97	0.02	0.25	21.95	166.99	23.64	4.69

The whole water–rock interaction process by which the speleothems of Xueyu Cave are generated can be summarized as the equation below:

$$\mathrm{CaCO_{3(host-rock)}} + \mathrm{H_2O_{(precipitation)}} + \mathrm{CO_{2(soil)}} \leftrightarrow \mathrm{Ca^{2+}} + 2\mathrm{HCO_3^-}_{\mathrm{(drip-water)}} \leftrightarrow \mathrm{CaCO_3}\downarrow_{\mathrm{(speleothem)}} + \mathrm{H_2O} + \mathrm{CO_2}\uparrow \quad (1)$$

In Eq. (1), the host rocks provide cation (e.g., Ca^{2+}) sources to the interaction, water is from precipitation, and soil acts as the main CO_2 source. After the first water–rock interaction step, the leachate is formed and begins to percolate downward; during the percolating processes, more substance of the host rock is taken into the solutions, and when the leachate arrives, the cave chambers sharply drawn down of the pCO_2 lead to the supersaturation of the solution, and then speleothems precipitate from the drip waters.

Therefore, the host rock acts as the cation source of the drip waters, and water is used as a medium to control the mineral and chemical components of speleothems. The investigation

on lithology and chemical compositions of host rocks show their predominant mineral component is LMC, indicating the drip waters likely have low Mg/Ca ratio and the mineral components of speleothems are very likely to be predominated by LMC. This hypothesis is supported by crystallographic characteristics of secondary calcite mineral; furthermore, the hypothesis is also supported by chemical composition data of drip waters and speleothems.

The hydrochemical characteristics of drip waters in Xueyu Cave show an obviously seasonal variation; besides, the precipitation rate of cave sediments also shows a seasonal variation, and investigation data reveals the monthly mean values of precipitation rate of cave sediments in post-monsoon season and pre-monsoon season are 0.45 and 0.25 g, respectively. Cai et al. (2011) interpreted that this phenomenon may be caused by the seasonal recharge regime of drip water, but we think the recharge regime of drip water is not the only reason. In fact, in monsoon regions, not only the precipitation but also the concentration of soil CO_2 varies seasonally, and they are both important controls on the seasonal variation phenomenon of hydrochemistry of drip water and precipitation rate of cave sediments.

In summary, the internal relations of the host rock, drip water, and speleothems of Xueyu Cave can be demonstrated as a conceptual model (Fig. 13). In post-monsoon season, much precipitation and high temperature strengthen the metabolism of organisms, resulting in the generation of large quantity of CO_2 and reducing the pH of soil water; besides, the large amount of precipitation also leads to the rising of the water table and speeds up the water cycle of the cave system. These factors significantly strengthen the water–rock interaction between the host rock and percolating water, leading to the drip waters of relatively higher Ca^{2+} and HCO_3^- content and lower pH and eventually accelerating the precipitation of speleothems. In pre-monsoon season, the decrease of temperature and precipitation amount lowers the metabolism of organisms and the circulation rate of ground water, resulting in lower Ca^{2+} and HCO_3^- content and higher pH and Mg/Ca and eventually reducing the precipitation rate of speleothems. Although the main geochemical indexes vary seasonally, due to the predominant mineral component of host rock is LMC, the speleothems mainly consist of LMC and the Mg/Ca ratio remains stable.

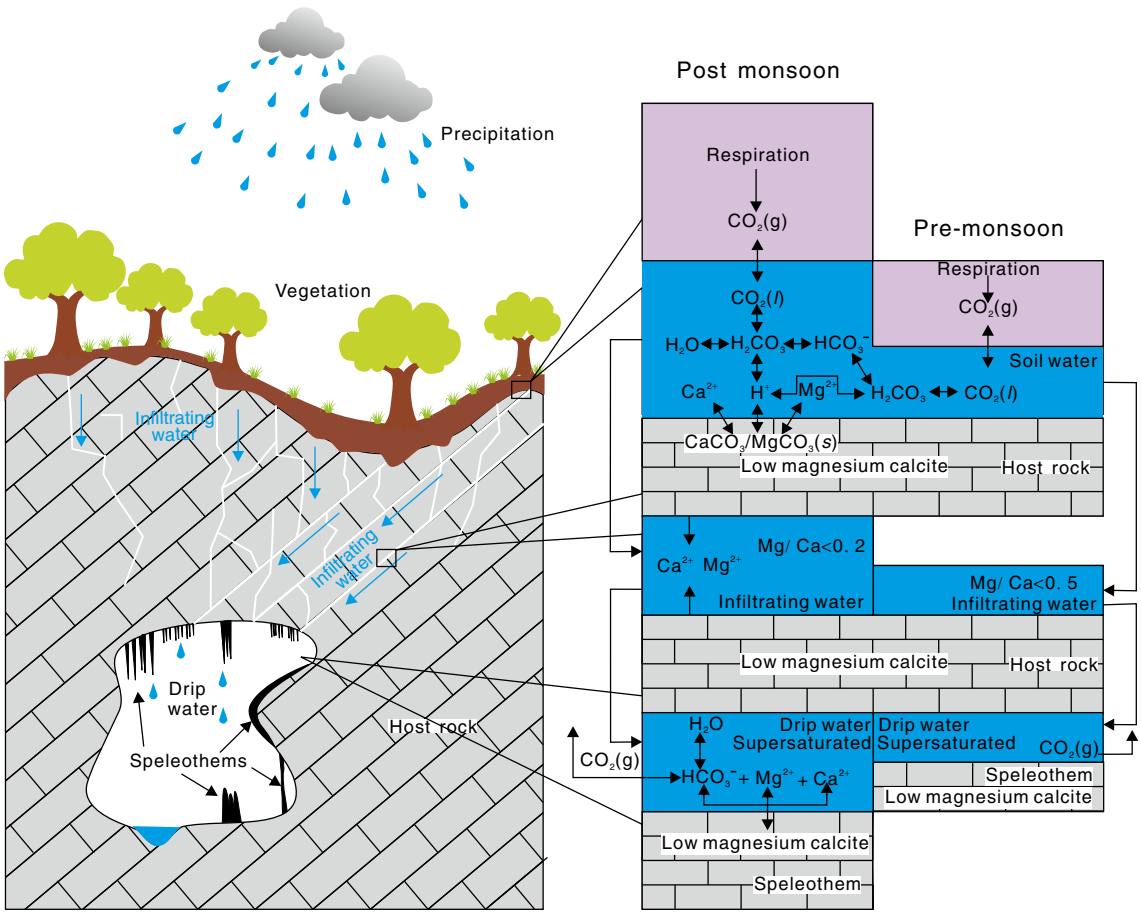

Fig. 13 Conceptual model of the internal relations of the host rock, drip water, and speleothems of Xueyu Cave. The *thickness of purple squares* represents the concentration of soil CO_2, the *thickness of blue squares* represents the quantity of water, and *the thickness of squares of brick stripes* and *speleothem marks* represent the precipitation rate of the speleothems

Conclusions

This study focused on links between the host rock, drip water, and speleothems of Xueyu Cave, based on the investigation on petrology and geochemistry of host rock and speleothems and hydrochemical characteristics of drip water; some conclusions are revealed as follows:

1. The host rock of Xueyu Cave have suffered meteoric water diagenesis, resulting in universal sparry LMC cementation and significantly reducing the Mg content in the host rock.
2. The monsoon climate drives precipitation and the soil CO_2 concentration, which will change the intensity of water–rock interaction and result in the obviously seasonal variation of chemical characteristics of drip waters.
3. Due to the predominant mineral components of the host rock are LMC, the drip water and speleothems have low Mg/Ca ratios too.
4. In the KDS of Xueyu Cave, the host rock acts as the main material source of drip water and speleothems, and water is used as the media to impact the mineral and chemical components of speleothems.

Acknowledgments The authors are grateful to Prof. Daoxian Yuan at the Institute of Karst Geology, Chinese Academy of Geological Sciences and Prof. Zaihua Liu at the Chinese Academy of Sciences, for they gave some crucial comments and advices on this study. The authors are also grateful to the teachers and students of the Laboratory of Isotopic Geochemistry, Southwest University, for their help with the analysis. This study was supported by the National Natural Science Foundation of China (Grant No. 41272135, No. 41302213, and No. 41302023); Karst Dynamics Laboratory, Ministry of Land and Resources, China; and Guangxi Zhuang Autonomous Region, China (Grant No. KDL2011-04).

References

Bar-Matthews M, Matthews A, Ayalon A (1991) Environmental controls of speleothem mineralogy in a karstic dolomitic terrain (Soreq Cave, Israel). J Geol 99(2):189–207

Cacchio P, Contento R, Ercole C, Cappuccio G, Martinez MP, Lepidi A (2004) Involvement of microorganisms in the formation of carbonate speleothems in the Cervo Cave (L'Aquila-Italy). Geomicrobiol J 21:497–509

Cai B, Zhu J, Ban F, Tan M (2011) Intra-annual variation of the calcite deposition rate of drip water in Shihua Cave, Beijing, China and its implications for palaeoclimatic reconstructions. Boreas 40(3):525–535. doi:10.1111/j.1502-3885.2010.00201.x

Choudens-Sanchez VD, Gonzalez LA (2009) Calcite and aragonite precipitation under controlled instantaneous supersaturation: elucidating the role of CaCO3 saturation state and Mg/Ca ratio on calcium carbonate polymorphism. J Sediment Res 79:363–376

Contos AK, James JM, Heywood B, Pitt K, Rogers P (2001) Morphoanalysis of bacterially precipitated subaqueous calcium carbonate from Weebubbie Cave, Australia. Geomicrobiol J 18:331–343

Davis KJ, Dove PM, Wasylenki LE, De-Yore JJ (2004) Morphological consequences of differential Mg2+ incorporation at structurally distinct steps on calcite. Am Mineral 89:714–720, 0003-004X/04/0506-714

Fairchild IJ, Borsato A, Tooth AF, Frisia S, Hawkesworth CJ, Huang Y, McDermott F, Spiro B (2000) Controls on trace element (Sr-Mg) compositions of carbonate cave waters: implications for speleothem climatic records. Chem Geol 166:255–269

Folk RL (1974) The natural history of crystalline calcium carbonate: effect of magnesium content and salinity. J Sediment Petrol 44(1):40–53

Ford DC, Williams PW (2007) Karst hydrogeology and geomorphology. John Wiley and Sons, Chichester, 562 p

Forti P (2001) Biogenic speleothems: an overview. Int J Speleol 30(A (1/4)):39–56

Frisia S, Borsato A, Fairchild IJ, Mcdermott F, Selmo EM (2002) Aragonite-calcite relationships in speleothems (Grotte de Clamouse, France): environment, fabrics, and carbonate geochemistry. J Sediment Res 72(5):687–699

Gascoyne M (1983) Trace element partition coefficients in the calcite–water system and their paleoclimatic significance in cave studies. J Hydrol 61:213–222

Gibbs RJ (1970) Mechanisms controlling world water chemistry. Science 170(3963):1088–1090

Gonzalez LA, Lohmann KC (1987) Controls on mineralogy and composition of spelean carbonates: Carlsbad Cavern, New Mexico. In: James NP, Choquette PW (eds) Paleokarst. Springer, New York, pp 81–101

Holland HD, Kirsipu TW, Huebner JS, Oxburgh UM (1964) On some aspects of the chemical evolution of cave waters. J Geol 72:36–67

Huang S (2010) Carbonate diagenesis. Geological Publish House, Beijing, 288p (in Chinese)

Huang S, Zhang M, Sun S, Hu Z, Wu S, Pei C (2006) Age calibration of carbonate samples from the Triassic Feixianguan Formation, Well Luojia 2, Eastern Sichuan by strontium isotope stratigraphy. J Chengdu Univ Technol (Sci Technol Ed) 33(2):111–116 (in Chinese with English abstract)

Huang S, Qing H, Huang P, Hu Z, Wang Q, Zou M, Liu H (2008) Evolution of strontium isotopic composition of seawater from Late Permian to Early Triassic based on study of marine carbonates, Zhongliang Mountain, Chongqing, China. Sci China Ser D Earth Sci 51(4):528–539

Lahann RW (1978) A chemical model for calcite crystal growth and morphology control. J Sediment Petrol 48(1):337–344

Longman MW (1980) Carbonate diagenetic textures from nearsurface diagenetic environments. AAPG Bull 64(4):461–487

Moore GW (1952) Speleothem—a new cave term. Natl Speleol Soc News 10(6):2

Musgrove M, Banner JL (2004) Controls on the spatial and temporal variability of vadose dripwater geochemistry: Edwards aquifer, central Texas. Geochim Cosmochim Acta 68:1007–1020

Onac BP, Forti P (2011a) State of the art and challenges in cave minerals studies. Studia UBB Geol 56(1):33–42

Onac BP, Forti P (2011b) Minerogenetic mechanisms occurring in the cave environment: an overview. Int J Speleol 40(2):79–98

Oster JL, Montanez IP, Kelley NP (2012) Response of a modern cave system to large seasonal precipitation variability. Geochim Cosmochim Acta 91:92–108

Parkhurst DL, Appelo CAJ (1999) User's guide to PHREEQC (version 2)—a computer program for speciation, batch-reaction, one-dimensional transport, and inverse geochemical calculations. USGS, Water-Resources Investigations Report 99–4259: 326p. http://www.xs4all.nl/~appt/index.html

Piper AM (1944) A graphic procedure in the geochemical interpretation of water-analyses. Am Geophys Union 25(6):914–928. doi:10.1029/TR025i006p00914

Pu J, Shen L, Wang A, He Q, Yuan W, Hu Z, Chen B, He Y (2009) Space-time variation of hydro-geochemistry index of the Xueyu cave system in Fengdu county, Chongqing. Carsologica Sin 28(1):49–54 (in Chinese with English abstract)

Scholle PA, Ulmer-Scholle DS (2003) A color guide to the petrology of carbonate rocks: grains, textures, porosity, diagenesis. Published by The American Association of Petroleum Geologists Tulsa, Oklahoma, U.S.A.: 461p

Self CA, Hill CA (2003) How speleothems grow: an introduction to the ontogeny of cave minerals. J Cave Karst Stud 65(2):130–151

Spotl C, Fairchild IJ, Tooth AF (2005) Cave air control on dripwater geochemistry, Obir Caves (Austria): implications for speleothem deposition in dynamically ventilated caves. Geochim Cosmochim Acta 69(10):2451–2468

Stanley SM, Ries JB, Hardie LA (2002) Low-magnesium calcite produced by coralline algae in seawater of Late Cretaceous composition. PNAS 99(24):15323–15326

Tămas T, Kristály F, Barbu-Tudoran L (2011) Mineralogy of Iza Cave (Rodnei Mountains, N. Romania). Int J Speleol 40(2): 171–179

Thrailkill J (1971) Carbonate deposition in Carlsbad caverns. J Geol 79: 683–695

Toran L, Roman E (2006) CO2 outgassing in a combined fracture and conduit karst aquifer near Lititz Spring, Pennsylvania. Geol Soc Am Spec Pap 404(23):275–282

Wang Z, Zhang J, Li T, Xie G, Ma Z (2010) Structural analysis of multi-layer detachment folding in eastern Sichuan Province. Acta Geol Sin 84(3):479–514

Wang Z, Zhang J, Li T, Zhou X, Ma Z, Tang L, Xiao W, Yan X (2012) Structural traps in detachment folds: a case study from comb- and trough-like deformation zones, east Sichuan, China. Acta Geol Sin 86(4):828–841

Xu S, Yin J, Wang X, Yang P, Mao H, Shen L (2012) Impact of seasonal karstfication on the precipitation rate of cave sediments: a case study of the underground river system of the Xueyu Cave, Chongqing. Trop Geogr 32(5):481–486

Yuan D, Liu Z, Lin Y, Shen J, He S, Xu S, Yang L, Li B, Qing J, Cai W, Cao J, Zhang M, Jiang Z, Zhao J (2002) Karst dynamic system of China. Geological Publish House, Beijing, 275p. (in Chinese)

Zharkov MA, Chumakov NM (2001) Paleogeography and sedimentation settings during Permian–Triassic reorganizations in biosphere. Stratigr Geol Correl 9(4):340–363

Zhu X, Zhang Y, Han D, Wen R, Chen B (2004) Cave characteristics and speleothems in Xueyu cave group, Fengdu, Chongqing City. Carsologica Sin 23(2):85–90 (in Chinese with English abstract)